Supporting Information

Visualization of Pathway Usage in an Extended Carbohydrate Conversion Network Reveals the Impact of Solvent Enabled Proton Transfer

Pernille R. Jensen,[‡] *Rikke K. Knudsen,*[§] *and Sebastian Meier*[§*]

[‡]Technical University of Denmark, Department of Health Technology, Ørsteds Plads 349, 2800-Kgs. Lyngby, Denmark

[§]Technical University of Denmark, Department of Chemistry, Kemitorvet Building 207, 2800-Kgs. Lyngby, Denmark

*Email semei@kemi.dtu.dk

SI Contents (16 pages, 15 figures):

Supplementary Figures:

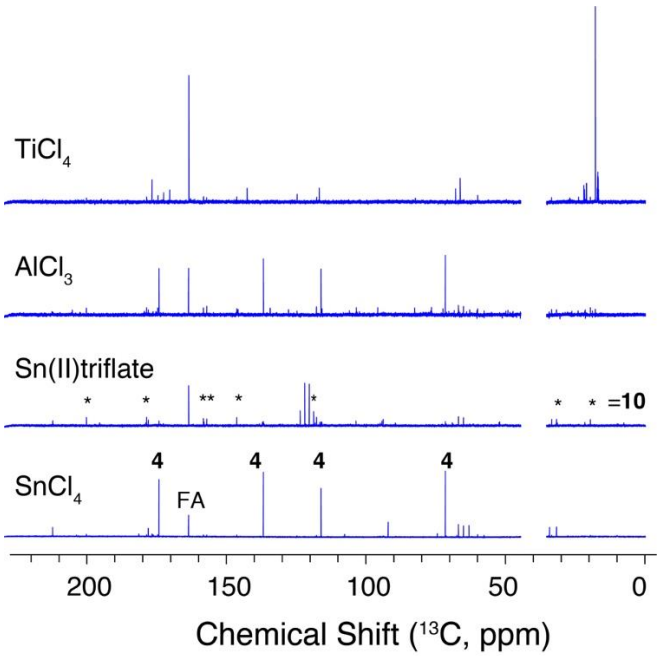

Figure S1. Post-reaction material upon conversion of erythrulose (40 mg) by various Lewis acidic salts (12:1 substrate to catalyst ratio) at 353 K in d_6-DMSO (550 µl), overnight.

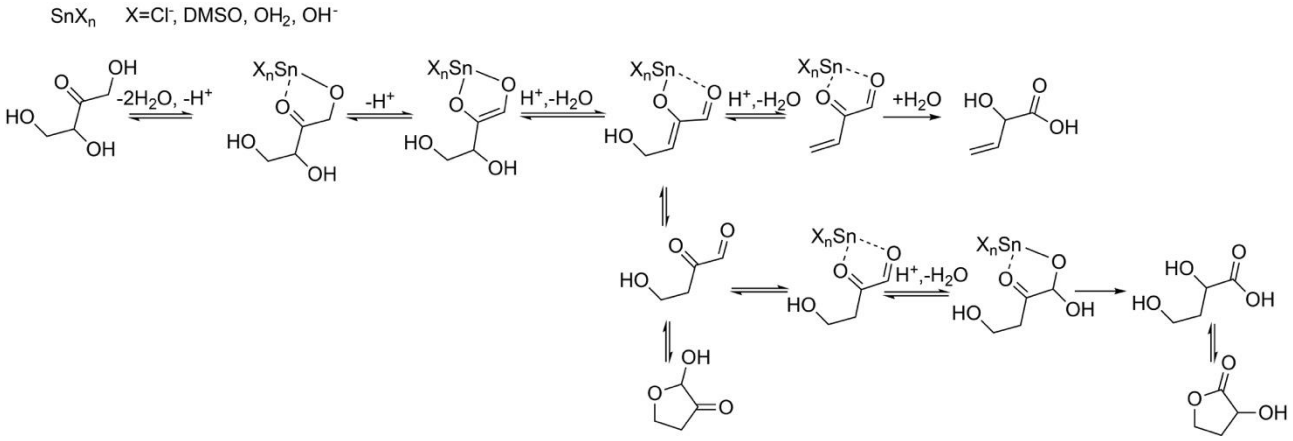

Figure S2. Plausible function of the Sn(IV) catalyst center in the reaction pathway. Complexes between the metal center and the substrate or intermediates remain to be experimentally characterized, as transient binding and low complex populations necessitate future method developments.

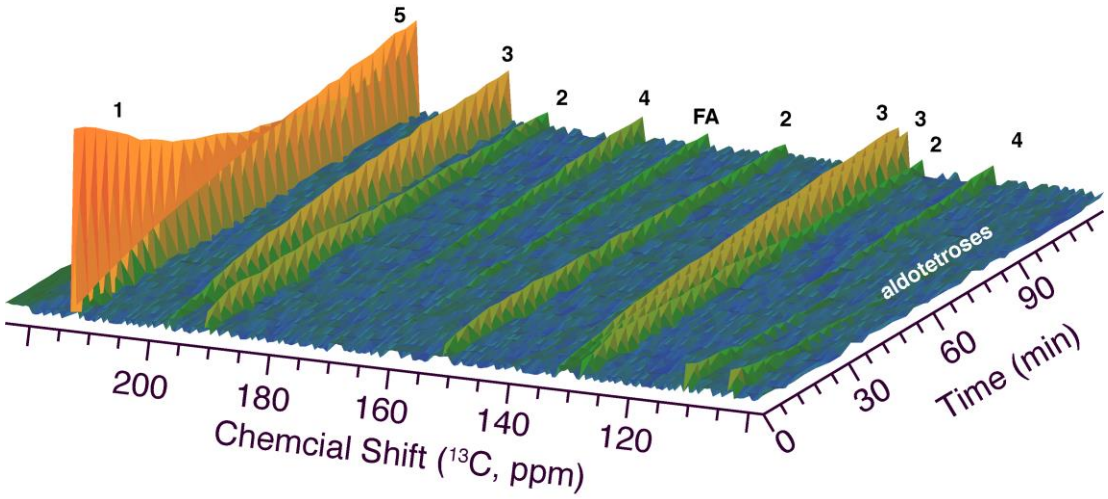

Figure S3. Time course of erythrulose conversion depicting aldotetrose (erythrose and threose) signals alongside other chemicals. Minor populations of aldotetroses share the kinetic profile of the ketose substrate **1**. All tetrose species were therefore treated as an interconverting pool and the integrals were summed up for the reaction progress curves of substrate conversion. FA denotes formic acid. Reaction conditions: L-erythrulose (40 mg) and $SnCl_4 \cdot 5H_2O$ (10 mg) in d_6-DMSO (550 μL) at 313 K without addition of water.

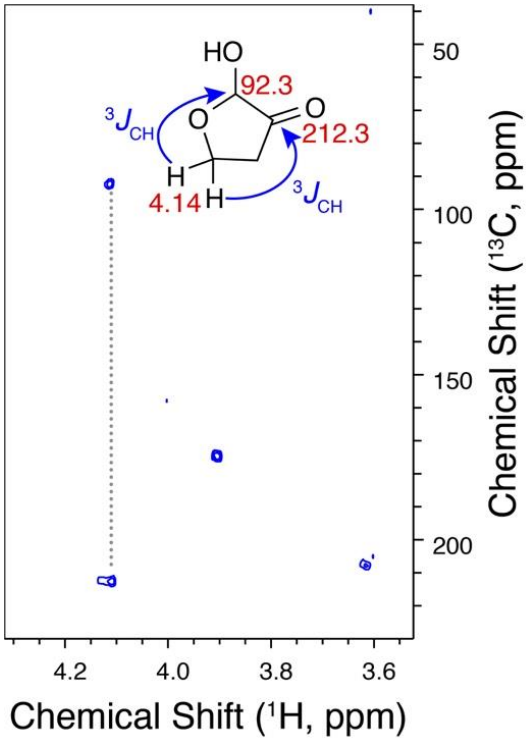

Figure S4. ^{1}H-^{13}C HMBC of a reaction mixture, showing the cyclic structure of the predominant 3-deoxythreosone compound **5.** Long range connections from H4 to hemiacetal and keto group via 3JCH couplings are show and indicated by blue arrows. Reaction conditions: L-erythrulose (40 mg) and $SnCl_4 \cdot 5H_2O$ (10 mg) in d_6-DMSO (550 μl) at 313 K, overnight.

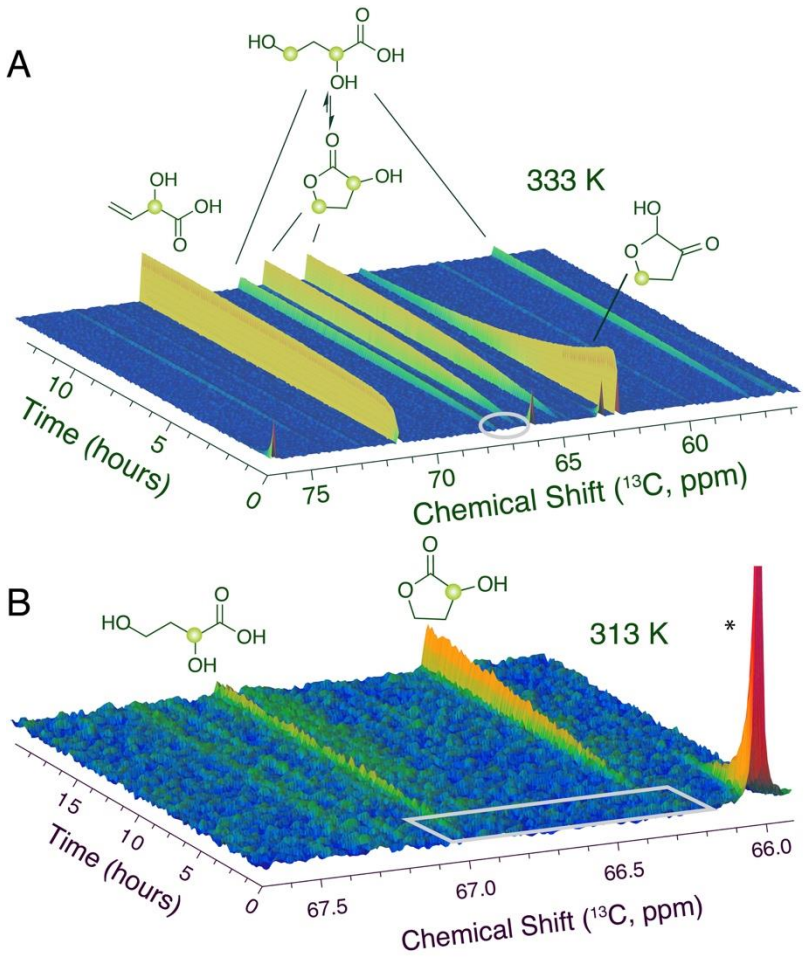

Figure S5. Time series of ^{13}C NMR spectra of cyclic and acyclic α-hydroxyesters **6** and **9** at 333 K (A) and 313 K (B). Signals of erythrulose substrate are labelled by asterisks. Spectra show that the acyclic compound **9** is detectable prior to the equilibration with its cyclic counterpart **6** at both temperatures (highlighted by grey boxes). Reaction conditions: L-erythrulose (40 mg) and $SnCl_4 \cdot 5H_2O$ (10 mg) in d_6-DMSO (550 μL) at 333 K or 313 K.

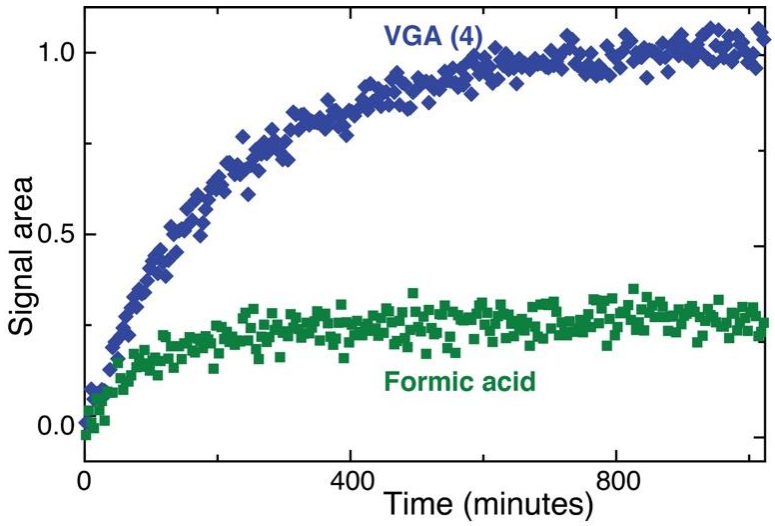

Figure S6. Kinetic profiles of VGA and formic acid formation indicate that formic acid may form in competition with the formation of VGA from from vinylglyoxal (**3**). Such a mechanism paralles the proposed mechanism for the conversion of a β, γ-unsaturated α-hydroxy-carbonyl intermediate in the conversion of HMF to levulinic acid and formaic acid. Reaction conditions: L-erythrulose (40 mg), $SnCl_4 \cdot 5H_2O$ (10 mg) in d_6-DMSO/D_2O (85%/15% v/v, total 550 μL) at 313 K.

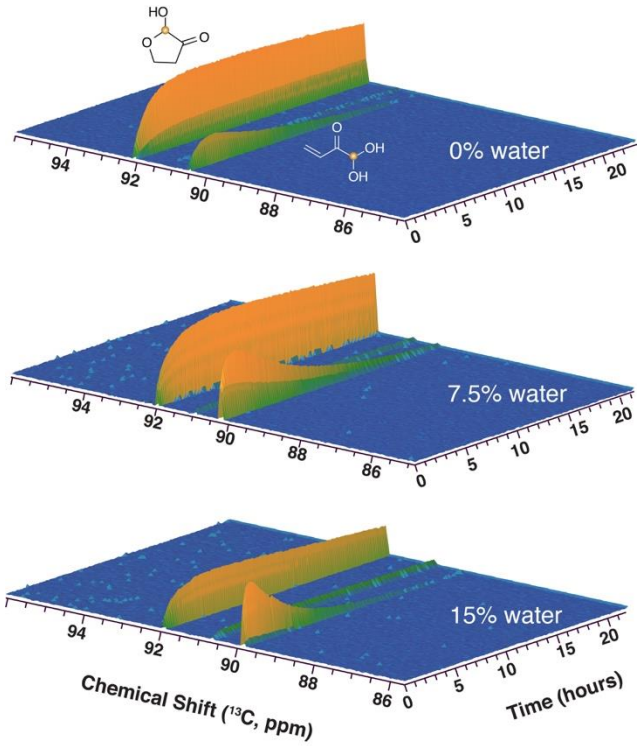

Figure S7. Reaction progress curves towards intermediates **3** and **5** at varying water content in DMSO. Experiments correspond to the experiments of main text Figure 6. Kinetic profiles indicate that **3** and **5** form in parallel in the absence of added water, while the addition of water favors a more rapid flux towards the hydrate of vinylgloxal **3**. Changes in reaction profiles are consistent with a change of reaction control at the branch point (**2** to **3** or **5**) from predominantly kinetic control (in the absence of water) to predominantly thermodynamic control (upon addition of water). Reaction conditions: L-erythrulose (27 mg) and $SnCl_4 \cdot 5H_2O$ (10 mg) in d_6-DMSO/D_2O of the indicated ratio (v/v added water, total 550 μL) at 313 K.

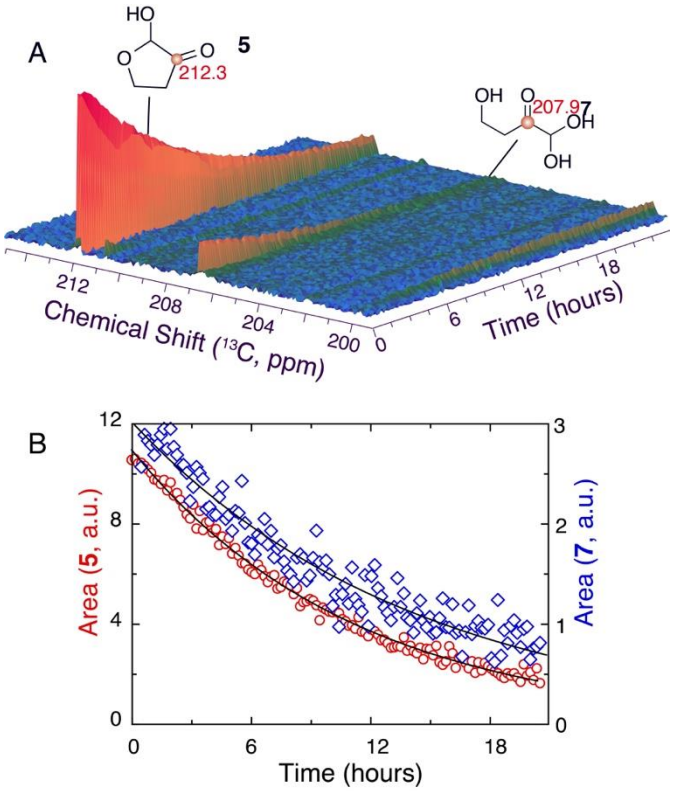

Figure S8. Series of ^{13}C NMR spectra (A) and corresponding signal areas (B) for cyclic and acyclic 3-deoxythreosone intermediates **5** and **7** at varying water content in DMSO. Time series data indicate conversion with comparable kinetics due to equilibration of both forms under the reaction conditions, indicating that **7** is formed from **5**, not from rehydration of **3**. Reaction conditions: L-erythrulose (40 mg), and $SnCl_4 \cdot 5H_2O$ (10 mg) in d_6-DMSO/D_2O (30% added water, total 550 μL) at 333 K.

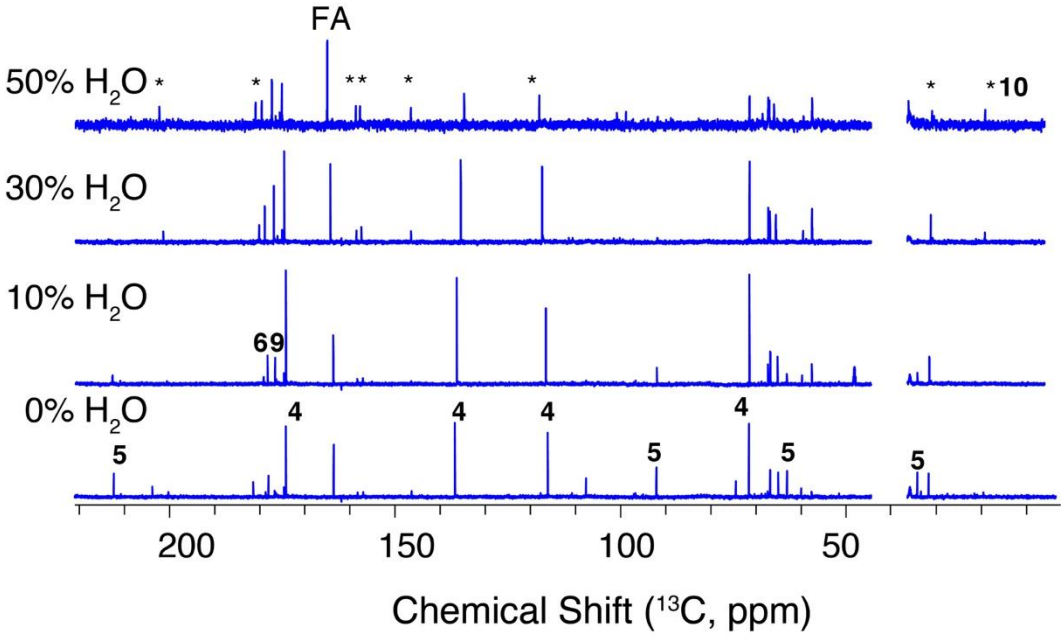

Figure S9. ^{13}C NMR spectra of post reaction material for reactions with varying water content and added Brønsted acid. Reaction conditions: L-erythrulose (40 mg) and $SnCl_4 \cdot 5H_2O$ (10 mg) in d_6-DMSO/D_2O (v/v as indicated, 550 μL) at 363 K for 90 minutes. Asterisks indicate erythropyrone (**10**) signals.

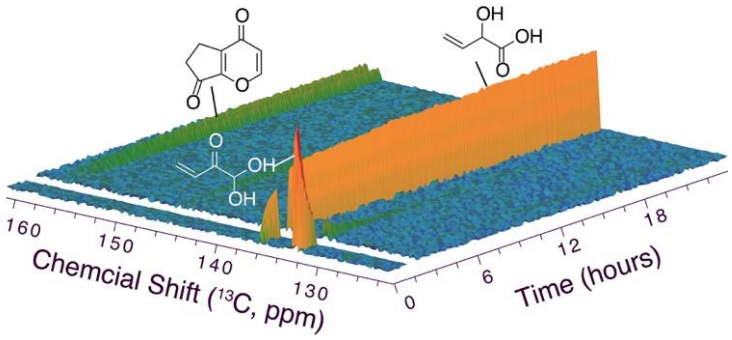

Figure S10. Time series of ^{13}C NMR spectra showing the kinetics of erythropyrone formation upon accumulation of acidic product with a slow kinetics similar to the kinetics of oligomerization deduced in main text Figure 4. The experiment was interrupted after 80 minutes in order to acquire assignment spectra and validate structure determinations. Reaction conditions: L-erythrulose (40 mg) and $SnCl_4 \cdot 5H_2O$ (10 mg) in d_6-DMSO/D_2O (30% added water in a total volume of 550 μL) at 333 K.

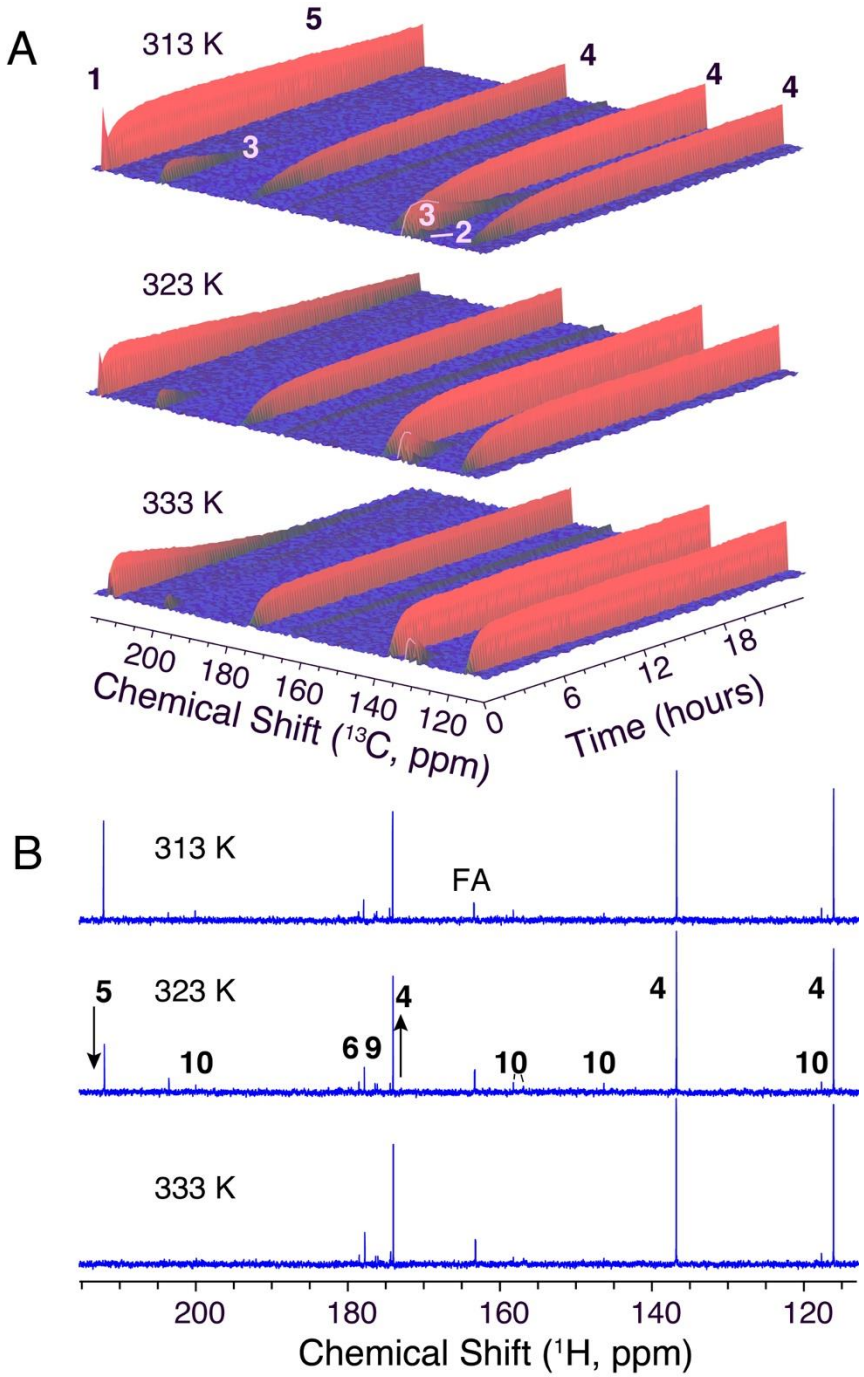

Figure S11. Series of ^{13}C NMR spectra (A) and ^{13}C NMR spectra of post reaction material (B) at varying temperature. Reaction conditions: L-erythrulose (40 mg) and $SnCl_4 \cdot 5H_2O$ (10 mg) in d_6-DMSO (550 μL). Spectra of panel (B) are taken after 40 hours (313 K) and 24 hours (323 K and 333 K), respectively.

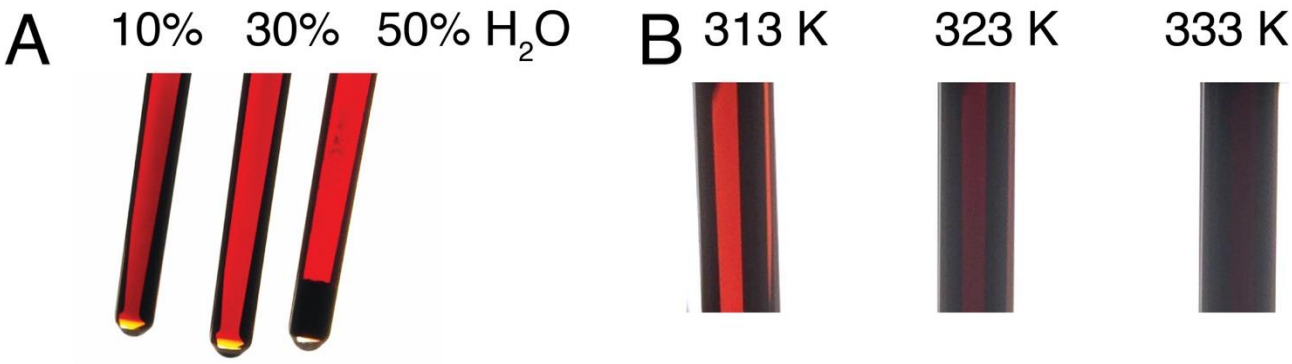

Figure S12. Photographs of (A) post-reaction material after the experiments of Figure S9 (water effect) and (B) post-reaction material after the *in situ*-experiments of Figure S11 (temperature effect) show increased humin formation at higher water contents and at higher temperature.

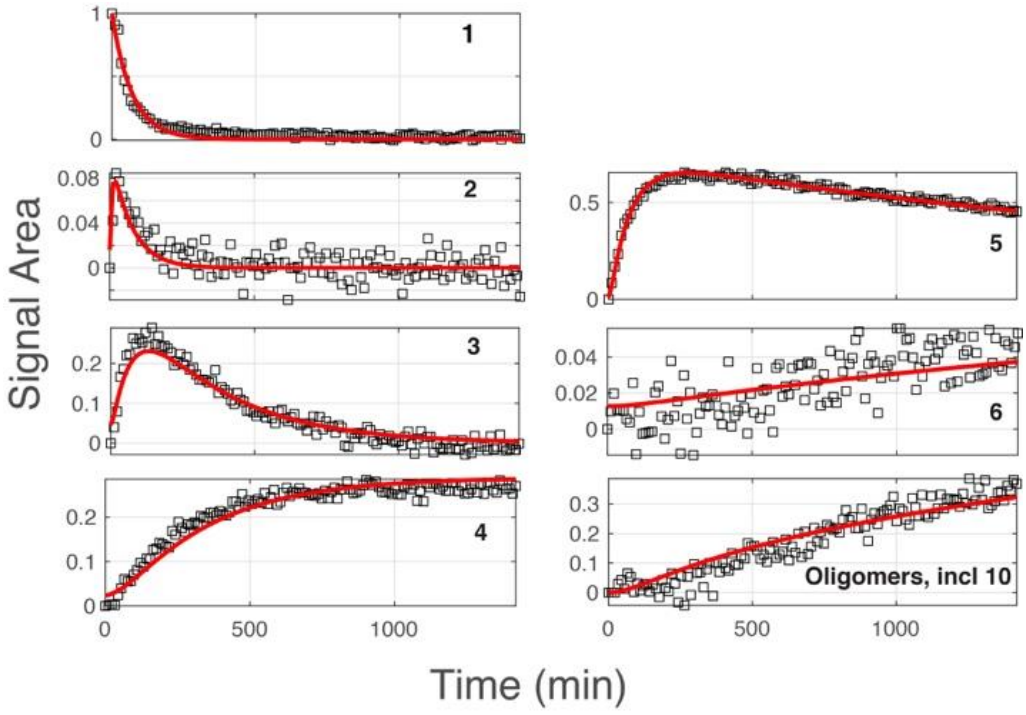

Figure S13. Experimental ^{13}C NMR integrals of compounds **1-6** and a kinetic fit resembling Scheme 1 and Figure 5 shown in red. The figure resembles main text Figure 4, but adjusts the ordinate axis (signal areas) to demonstrate the quality of the fit also for minor molecular species, especially **2** and **6**. Red lines depict from kinetic modelling calculations.

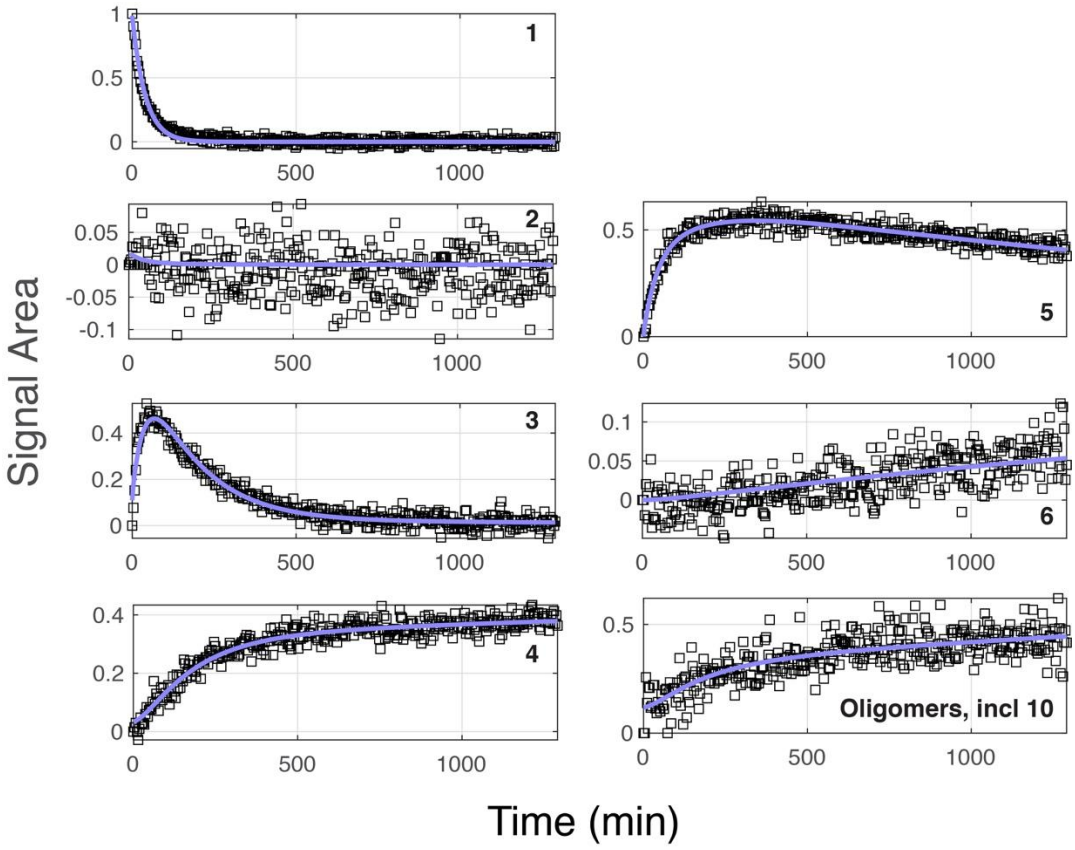

Figure S14. ^{13}C NMR integrals of compounds **1**-**6** and a kinetic fit (blue curves and blue values in main text Figure 5) using the experimental data of Figure 6 in the presence of 15% (v/v) water. Lines depict kinetic modelling calculations.

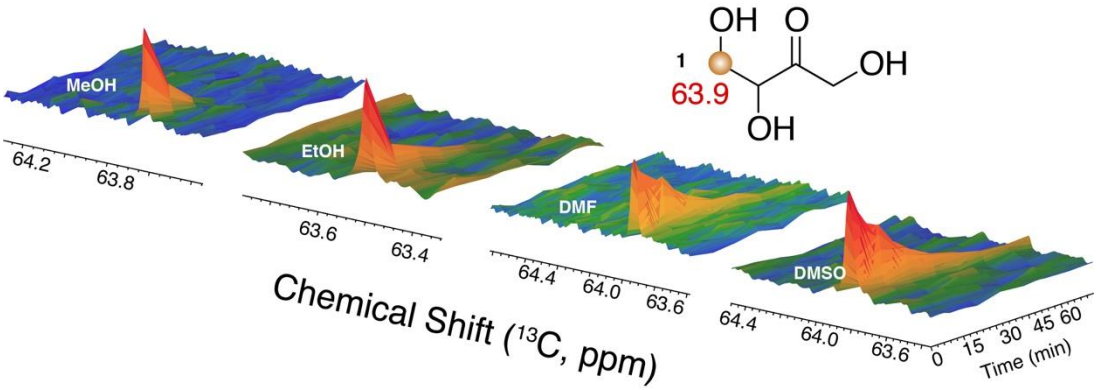

Figure S15. Reaction progress in various alcohols and aprotic polar solvents (experiments of main text Figure 8). Conversion of the substrate is shown, indicating a faster conversion in alcohols than in DMF and DMSO. Reaction conditions: L-erythrulose (40 mg) and $SnCl_4 \cdot 5H_2O$ (10 mg) in 550 µL d_6-DMSO, protonated DMF containing 5% d_6-DMSO, methanol or ethanol containing 5% (v/v) d_4-methanol at 333 K.